



# Cu<sup>0</sup>NPs@CMC: an efficient recoverable nanocatalyst for decarboxylative A3 and A3 couplings under neat condition

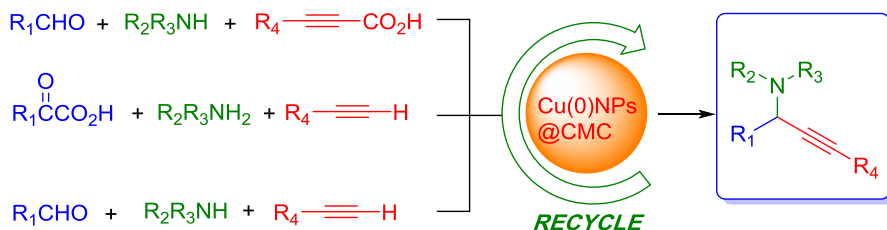
Xiaoping Liu<sup>1</sup> · Xiaobin Tan<sup>1</sup> · Yuemin Zhou<sup>1</sup> · Yiqun Li<sup>1,2</sup> · Zhubao Zhang<sup>1</sup>

Received: 11 December 2018 / Accepted: 2 March 2019  
© Springer Nature B.V. 2019

## Abstract

Copper nanoparticles assembled on carboxymethylcellulose (Cu<sup>0</sup>NPs@CMC) were successfully synthesized and well characterized by FT-IR, SEM, EDS, TEM, XPS, and ICP-AES. The new prepared nanocatalyst was applied effectively as a heterogeneous catalyst for the synthesis of propargylamines via decarboxylated A3 and classic A3 reaction under solvent-free condition. A broad spectrum of diversely polysubstituted propargylamines could be obtained in moderate to excellent yields. The present method showed several merits such as easy work-up, short reaction time, additive-free characteristic, solvent-free condition, functional group tolerance, usage of recyclable green and sustainable nanocatalyst.

## Graphical abstract



**Keywords** Carboxymethylcellulose · Copper nanoparticles · Decarboxylative A3 reaction · A3 reaction · Solvent-free condition

**Electronic supplementary material** The online version of this article (<https://doi.org/10.1007/s11164-019-03795-3>) contains supplementary material, which is available to authorized users.

✉ Zhubao Zhang  
drubao@163.com

Extended author information available on the last page of the article

Published online: 14 March 2019

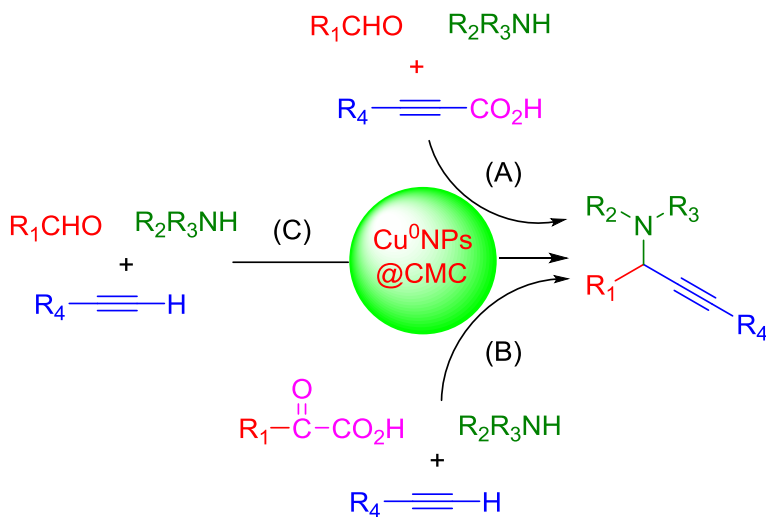
## Introduction

Propargylamines are one of the most widely used versatile synthetic building blocks for the construction of various biologically active, nitrogen-containing heterocyclic compounds and a key intermediate for the synthesis of complicated natural products and value-added chemicals [1–4]. They are also structural fragments presenting in natural products and potential therapeutic drug molecules [5–7]. Because of their unique biological and pharmaceutical properties, great effort has been made to synthesize these compounds. Conventionally, propargylamines are synthesized by nucleophilic addition of lithium acetylides, Grignard reagents, and organozinc reagents to imines or their derivatives [8–10]. However, in most cases, these methods often require stoichiometric amounts of organometallic reagents under harsh reaction conditions. An efficient alternative coupling of an aldehyde, an alkyne, and an amine (referred as A3 coupling) in the presence of homogeneous or heterogeneous transition metal catalysts has been developed [11–13]. These catalysts include homogeneous transition metal salts and complexes such as  $\text{Ag}^{\text{I}}$  [14–16],  $\text{Au}^{\text{I}}$  [17] and  $\text{Au}^{\text{III}}$  [18, 19],  $\text{Fe}^{\text{III}}$  [20, 21],  $\text{Zn}^{\text{II}}$  [22–24], and  $\text{Ru}^{\text{III}}/\text{Cu}^{\text{I}}$  bimetallic system [25], as well as heterogeneous catalysts such as  $\text{Fe}_3\text{O}_4@\text{SiO}_2$  [26], Ag(I)-functionalized MOF [27], Ag(I)-exchanged K10 montmorillonite clay [28], AuNPs- $\text{Fe}_3\text{O}_4$ -rGO [29], and core-shell Au@MOF-5 [30]. Recently, many A3 coupling reactions have been focused on using copper as a catalyst because copper is an abundant material and copper catalyst precursors are highly reactive, cheap, and easily available. Along this line, different homogeneous copper catalysts [31–35] and heterogeneous catalysts immobilized on different carriers [36–39] have been reported for A3 coupling reactions. Recently, great attention has been focused on the catalytic performance of transition metal NPs due to their high surface area-to-volume ratio. These nanocatalysts are considered to bridge the gap between homogeneous and heterogeneous catalysis. Thus, a number of CuNP catalysts have been employed for A3 coupling to synthesize propargylamine and is also well documented in the literature [40–44]. With the growing environmental concern, solvent-free organic synthesis has recently gained momentum from academia and industry. Therefore, rational design of solvent-free reactions is an important aim in the current research for the synthesis of propargylamines. Few reports using Cu catalysts have been reported for the synthesis of propargylamines under solvent-free conditions [40].

Similarly, decarboxylative A3-coupling is a practical transformation, wherein alkynyl carboxylic acids act as a stable surrogate to traditional organometallic reagents formed in situ decarboxylation. Efforts employing homogeneous catalysts such as CuI [45–47], CuBr [48, 49],  $\text{CuCl}_2/\text{CuI}$  [50],  $\text{CuI}/\text{Cu}(\text{OTf})_2$  [51], and heterogeneous catalysts including  $\text{CuO}/\text{Fe}_2\text{O}_3$  NPs [52], Cu(II)-hydromagnesite [53], and silica-embedded CuO nanospheres ( $\text{Cu}@\text{SiO}_2\text{-NS}$ ) [54] have been successfully done in decarboxylative A3 coupling reactions. Among the decarboxylative coupling reactions, copper-catalyzed methods are well studied and provide an attractive approach for the fabrication of propargylamines. Although homogeneous catalysts have many advantages including high reactivity, excellent

selectivity, and good yields, some drawbacks like tedious separation and reusability are encountered. In order to achieve recyclability of the catalysts, heterogeneous catalysts, especially supported nanocatalysts, have attracted much more attentions recently. However, Cu<sup>0</sup>NPs catalyzed decarboxylative strategies are rarely used in the decarboxylative A3 coupling reaction. Therefore, seeking new highly active and stable heterogeneous nanocatalyst is still demanded.

In recent years, using ecofriendly and biodegradable materials as supports for stabilization of metal nanoparticles has attracted great attention. Because of its widespread natural abundance and environmentally benign sustainable resource, sodium carboxymethylcellulose (Na@CMC) has become a green renewable alternative of currently used synthetic templates for metal nanoparticle synthesis. It is one of the most important cellulose derivatives with complete biodegradability, low cost and renewability, and can be regenerated from CO<sub>2</sub> and H<sub>2</sub>O via photosynthesis in the chlorophyll-containing cells. Na@CMC bearing carboxylic groups (–COO<sup>–</sup>Na<sup>+</sup>) and hydroxyl groups (–OH) on its cellulosic framework possess the potential to act as an excellent metallic cation exchange agent and ligand, which makes it a powerful support to immobilize metal nanoparticles via the interaction of ionic bonds and coordinated bonds between the counter metal cation species and polymer support [55]. More recently, we reported green ion exchange approach for the one-step preparation of Pd<sup>0</sup>NPs@CMC [56], Cu<sup>II</sup>-CMC@Fe<sub>3</sub>O<sub>4</sub> [57], assembled Pd<sup>0</sup>@Ce(OH)<sub>4</sub>/CMC [58], Pd<sup>0</sup>@CMC/Fe<sub>3</sub>O<sub>4</sub> [59], and CMC-Ce<sup>IV</sup> [60] to construct C–C bond and heterocycles. To the best of our knowledge there is no report on the decarboxylative A3 and A3 couplings using Cu<sup>0</sup>NPs@CMC nanocatalyst. With this background and in continuation of our interest towards green and sustainable nanocatalysis, we herein report the catalytic potential of Cu<sup>0</sup>NPs@CMC for decarboxylative A3 and A3 couplings under solvent-free conditions for the first time (Scheme 1).



**Scheme 1** Overview of Cu<sup>0</sup>NPs@CMC-catalyzed decarboxylative A3 (A and B) and classical A3 coupling (C)

## Experimental

### Chemicals and characterization

Fourier transform infrared spectra (FT-IR) were recorded on a Nicolet 6700 FT-IR spectrometer using KBr disc.  $^1\text{H}$  and  $^{13}\text{C}$  NMR spectra were recorded on a Bruker-300 Avance (300 MHz) instrument. The chemical shifts of  $^1\text{H}$  NMR and  $^{13}\text{C}$  NMR are reported in ppm relative to TMS (0.00 ppm) and  $\text{CD}_3\text{Cl}$  (77.0 ppm), respectively. Scanning electron microscopy (SEM) with energy-dispersive X-ray (EDX) were performed with a Zeiss Merlin instrument. Transmission electron microscopy (TEM) was conducted with a JEM 2100F instrument. Transmission electron micrograph (TEM) images were taken with a Philips Tecnai instrument. X-ray photoelectron spectroscopy (XPS) was performed on a Kratos Axis Ultra DLD spectrometer using Al X-ray source. The elemental copper content of the catalyst was determined by inductively coupled plasma-atomic emission spectrometry (ICP-AES) using Perkin Elmer Optima 2000 DV instrument. Thin-layer chromatography (TLC) analysis was performed on silica gel G/GF 254 plates. The products were purified by preparative TLC.

All solvents and chemicals were obtained from commercial sources and were used without prior purification.

### Preparation of the hybrid $\text{Cu}^0\text{NPs@CMC}$ nanocatalyst

The general procedure used for the preparation of the hybrid  $\text{Cu}^{\text{II}}\text@CMC$  was described by our group previously [38]. The hydrazine hydrate solution (80%, 12 mL) was added by drops into the  $\text{Cu}^{\text{II}}\text@CMC$  (3 g) suspension for 15 min with vigorous stirring at room temperature. A black solid formed, which visually indicates the formation of  $\text{Cu}^0\text{NPs@CMC}$ . Then the mixture was allowed to further react for 12 h. After that, the solid was filtered, washed several times with deionized water, successively with acetone, and finally dried under vacuum resulting  $\text{Cu}^0\text{NPs@CMC}$  nanocatalyst. The Cu content was determined to be 2.34 mmol/g by ICP-AES.

### General procedure for the decarboxylative A3 coupling from 3-phenylpropionic acid

Aryl aldehyde **1** (1 mmol), secondary amine **2** (1.5 mmol) and 3-phenylpropionic acid **3** (1.5 mmol) were added into a 10-mL glass tube. The reaction vessel was sealed with a Teflon septum and stirred in preheated oil bath for 12 h at 120 °C. Upon completion of the reaction, the resulting reaction mixture was loaded on a preparative TLC and eluted with EtOAc/heptanes (1/6, v/v) to afford the desired product **6**.

## General procedure for A3 coupling and decarboxylative A3 coupling of 2-oxo-2-phenylacetic

The experimental procedures were followed according to that mentioned above.

**A3 coupling:** aryl aldehyde (1 mmol), amine (1.2 mmol), and alkyne (1.5 mmol) for 5 h at 100 °C.

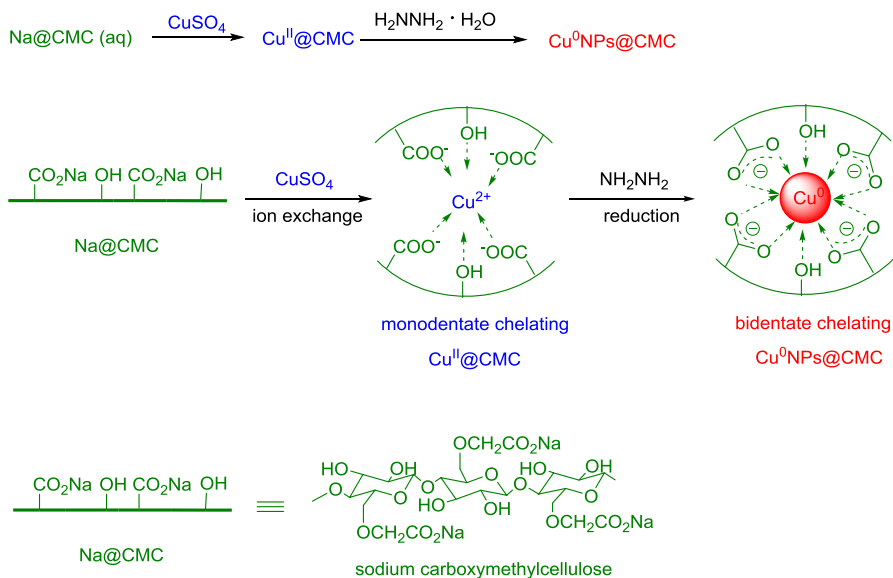
**Decarboxylative A3 coupling:** 2-oxo-2-phenylacetic acid (1 mmol), amine (1.2 mmol), and phenylacetylene (1.5 mmol) for 15 h at 110 °C.

## Results and discussion

### Preparation and characterization of Cu<sup>0</sup>NPs@CMC

The Cu<sup>0</sup>NPs@CMC nanocatalyst consisting of Cu<sup>0</sup>NPs and CMC matrix was prepared in two simple steps. In the first step, the Cu<sup>II</sup>@CMC was prepared via metathesis of Na@CMC with CuSO<sub>4</sub> following our previous work based on the property of Na@CMC being capable of exchanging with Cu<sup>II</sup> [38]. In the second step, the as-prepared Cu<sup>II</sup>@CMC was treated with hydrazine hydrate solution thoroughly for 12 h to afford the corresponding Cu<sup>0</sup>NPs based catalyst in which Cu<sup>0</sup>NPs assembled and nucleated on the CMC supports. The schematic illustration of the formation of the Cu<sup>II</sup>@CMC and Cu<sup>0</sup>NPs@CMC are shown in Scheme 2.

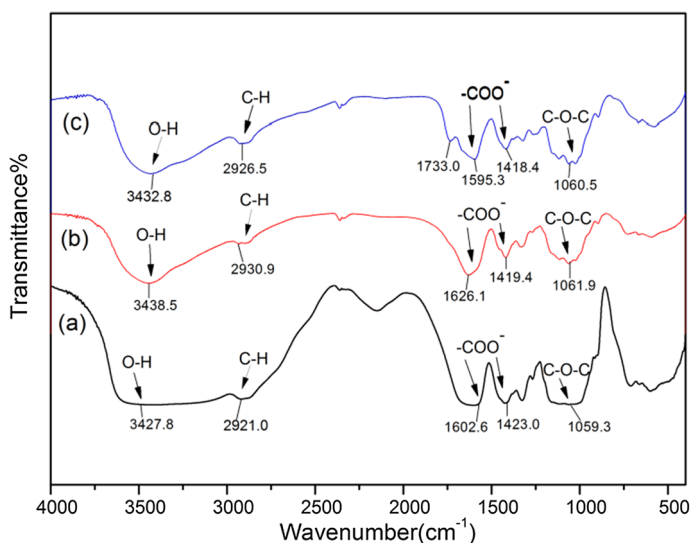
Then, the as-prepared Cu<sup>0</sup>NPs@CMC nanocatalyst was well characterized by FT-IR, SEM, EDX, TEM, and XPS techniques. The analytical data of the prepared copper nanoparticles were in good agreement with those reported.



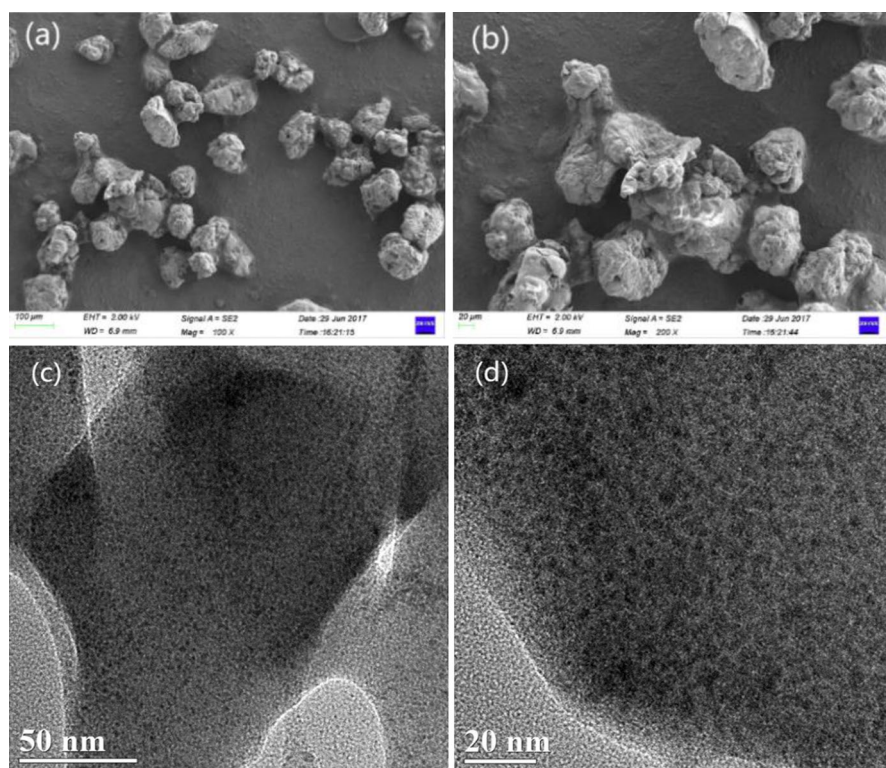
**Scheme 2** The procedure for the preparation of Cu<sup>II</sup>@CMC and Cu<sup>0</sup>NPs@CMC

Figure 1 shows the FT-IR spectra for Na@CMC (curve a), Cu<sup>II</sup>@CMC (curve b), and Cu<sup>0</sup>NPs@CMC (curve c). In curve (a), a strong and broad absorption band at 3428 cm<sup>-1</sup> is related to the -OH group stretching vibrations. The characteristic peaks at 1602 cm<sup>-1</sup> and 1423 cm<sup>-1</sup> are assigned to the carboxylate (-COO<sup>-</sup>Na<sup>+</sup>) asymmetric and symmetric stretching vibration. The band at 1059 cm<sup>-1</sup> is assigned to the -CH<sub>2</sub>-O-CH<sub>2</sub>- ether bonds stretches. These absorb peaks are shifted to 3439 cm<sup>-1</sup>, 1626 cm<sup>-1</sup>, 1419 cm<sup>-1</sup>, 1062 cm<sup>-1</sup> (curve b) and 3433 cm<sup>-1</sup>, 1595 cm<sup>-1</sup>, 1418 cm<sup>-1</sup>, 1061 cm<sup>-1</sup> (curve c) correspondingly. These shifts imply coordination between Cu<sup>2+</sup>, Cu<sup>0</sup> with -COO<sup>-</sup>, -OH, and -CH<sub>2</sub>-O-CH<sub>2</sub>- groups. Notably, the wavenumber separation  $\Delta$  between the asymmetric  $\nu$  (-COO<sup>-</sup>) and symmetric  $\nu$  (-COO<sup>-</sup>) stretches can be used to identify the type of the interactions. Characteristically, the  $\Delta$  value lies on the scope of 200–320 cm<sup>-1</sup> for monodentate, 140–190 cm<sup>-1</sup> for bidentate bridging, and < 110 cm<sup>-1</sup> for chelating bidentate [56, 61, 62]. As can be seen from curve (b) and curve (c), the  $\Delta$  values of 207 cm<sup>-1</sup> and 177 cm<sup>-1</sup> were observed, and thus, it is clear that the mode of the carboxylate binding in Cu<sup>II</sup>@CMC and Cu<sup>0</sup>NPs@CMC are correlated to monodentate chelating and bidentate chelating mode correspondingly. Evidently, CMC can interact with Cu<sup>2+</sup>, Cu<sup>0</sup> via the -COO<sup>-</sup>, -OH, and -CH<sub>2</sub>-O-CH<sub>2</sub>- functional groups, the possible chemical structure of Cu<sup>II</sup>@CMC and Cu<sup>0</sup>NPs@CMC may be suggested and depicted in Scheme 2.

The morphology of the freshly prepared Cu<sup>0</sup>NPs@CMC was characterized by SEM. SEM images in Fig. 2 are presented at different magnifications. The SEM images (Fig. 2a, b) clearly show that all these Cu<sup>0</sup>NPs@CMC catalysts have similar microparticles microstructures in varying sizes and shapes have rough surface, which facilitates the better mass transfer and enlarges its contact area and thus increases catalytic activity. The TEM images of the Cu<sup>0</sup>NPs@CMC catalyst (Fig. 2c, d) shows the presence of



**Fig. 1** FT-IR spectra of Na@CMC (a), Cu<sup>II</sup>@CMC (b), and Cu<sup>0</sup>NPs@CMC (c)



**Fig. 2** SEM images of Cu<sup>0</sup>NPs@CMC (the bar scale is 100 μm and 20 μm at **a** and **b**) and TEM images of Cu<sup>0</sup>NPs@CMC (the bar scale is 50 nm and 20 nm at **c** and **d**)

extremely uniform CuNPs with an average size of 2–10 nm, well dispersed throughout the polymer matrix, and almost no aggregation of CuNPs is found.

The existence of metallic elements in the catalyst was also confirmed by energy-dispersive X-ray spectroscopy (EDS) coupled with the SEM, which showed the metallic elements Cu, and non-metallic elements C and O in Fig. 3. Obviously, the presence of these elements confirmed that Cu is successfully immobilized on the CMC matrix.

We studied the oxidation state of the Cu of the hybrid using X-ray photoelectron spectroscopy (XPS). As shown in Fig. 4, two intense doublet peaks corresponding to Cu 2p<sub>1/2</sub> and Cu 2p<sub>3/2</sub> at 935.02, 955.00 eV related to Cu<sup>II</sup> (Fig. 4a), and peaks at 932.61, 952.65 eV, which is typically attributed to Cu<sup>0</sup> (Fig. 4b), respectively [63, 64].

### Cu<sup>0</sup>NPs@CMC as a heterogeneous catalyst for one-pot three-component decarboxylative couplings

To evaluate the optimized condition, a model reaction of 4-methylbenzaldehyde **1a**, morpholine **2a**, and phenylpropionic acid **3** was explored using catalytic amount of the prepared Cu<sup>0</sup>NPs@CMC catalyst in various media at specific temperature. The



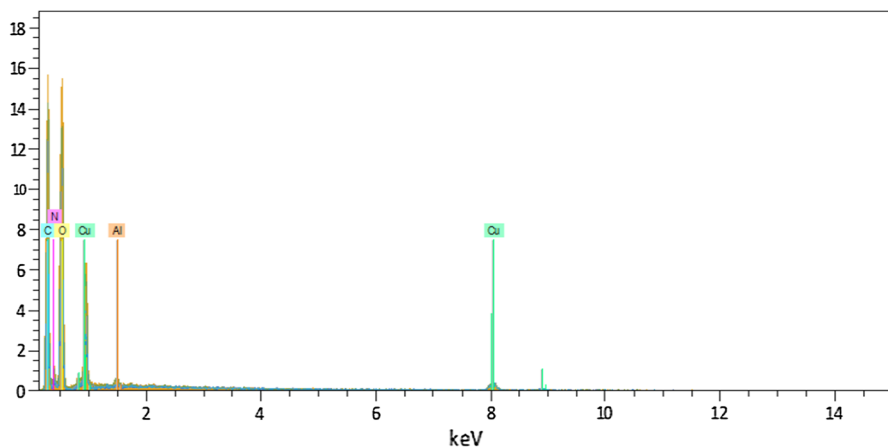


Fig. 3 EDS data for the fresh catalyst

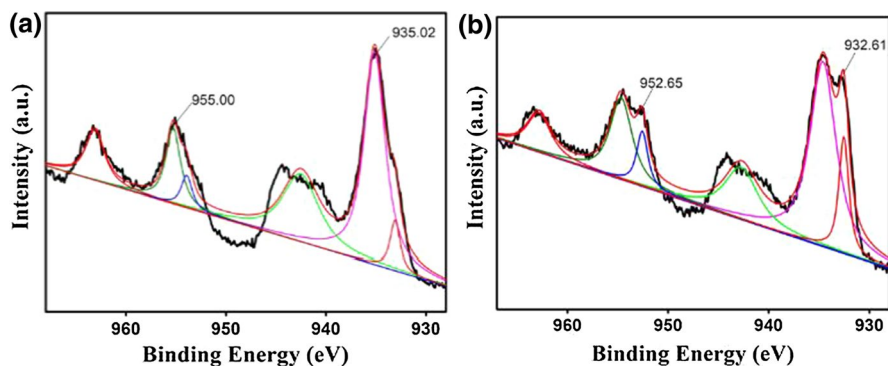
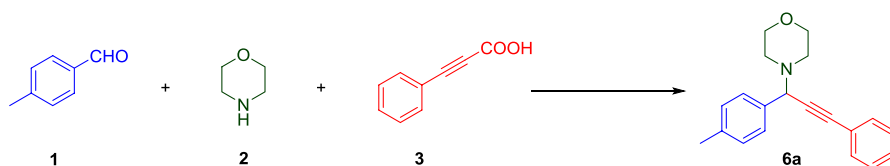


Fig. 4 Cu 2p XPS spectra of Cu<sup>II</sup>@CMC (a) and Cu<sup>0</sup>NPs@CMC (b)

results are summarized in Table 1. At the beginning, it is important to understand the role of Cu<sup>0</sup> NPs in the reaction. The most likely possibility is that Cu<sup>I</sup> and Cu<sup>II</sup> salts, as well as supported Cu<sup>II</sup> and Cu<sup>0</sup> are truly active species to catalyze the reaction. To prove this assumption, different copper salts such as CuSO<sub>4</sub>, Cu(OAc)<sub>2</sub>, CuCl, as well as supported Cu<sup>II</sup>@CMC, Cu<sup>0</sup>NPs@CMC, and even Na@CMC were investigated in the model reactions in toluene (Table 1, Entries 1–6). Among them, Cu<sup>0</sup>NPs@CMC gave the highest yield of 54% (Table 1, entry 6). When the reactions were performed in the presence of Na@CMC in toluene, a trace amount of product was formed (Table 1, entry 4). These results confirmed the catalytic role of the copper nanoparticles in the reaction. Subsequently, a variety of solvents were screened, a 54% yield of the desired product **6a** was observed in toluene using Cu<sup>0</sup>NPs@CMC as catalyst (Table 1, entry 6). THF, CH<sub>3</sub>CN, DMSO, EtOH, and H<sub>2</sub>O provide lower yields (Table 1, entries 7–11). Remarkably, the highest yield of **6a** was obtained when the reaction was carried out in neat condition (Table 1, entry 13). Then, we



**Table 1** Screening of the optimal parameters

Entry	Catalyst (mol%)	Solvent	Temp (°C)	Time (h)	Yield <sup>a</sup> (%)
1	CuSO <sub>4</sub> (20)	PhMe	100	24	31
2	Cu(OAc) <sub>2</sub> (20)	PhMe	100	24	40
3	CuCl (20)	PhMe	100	24	47
4	Na@CMC (7.5)	PhMe	100	24	Trace
5	Cu <sup>II</sup> @CMC (7.5)	PhMe	100	24	21
6	Cu <sup>0</sup> NPs@CMC (7.5)	PhMe	100	24	54
7	Cu <sup>0</sup> NPs@CMC (7.5)	THF	100	24	21
8	Cu <sup>0</sup> NPs@CMC (7.5)	CH <sub>3</sub> CN	100	24	22
9	Cu <sup>0</sup> NPs@CMC (7.5)	DMSO	100	24	27
10	Cu <sup>0</sup> NPs@CMC (7.5)	EtOH	100	24	30
11	Cu <sup>0</sup> NPs@CMC (7.5)	H <sub>2</sub> O	100	24	Trace
12	Cu <sup>II</sup> @CMC (7.5)	Neat	100	24	42
13	Cu <sup>0</sup> NPs@CMC (7.5)	Neat	100	24	53
14 <sup>b</sup>	Cu <sup>0</sup> NPs@CMC (7.5)	Neat	100	24	60
15 <sup>b</sup>	Cu <sup>0</sup> NPs@CMC (7.5)	Neat	110	24	63
16 <sup>b</sup>	Cu <sup>0</sup> NPs@CMC (7.5)	Neat	120	24	77
17 <sup>b</sup>	Cu <sup>0</sup> NPs@CMC (5)	Neat	120	24	53
18 <sup>b</sup>	Cu <sup>0</sup> NPs@CMC (10)	Neat	120	24	78
19 <sup>b</sup>	Cu <sup>0</sup> NPs@CMC (7.5)	Neat	120	15	78
20 <sup>b</sup>	Cu <sup>0</sup> NPs@CMC (7.5)	Neat	120	12	85
21 <sup>b</sup>	Cu <sup>0</sup> NPs@CMC (7.5)	Neat	120	9	77

Reaction conditions: **1a** (1 mmol), **2a** (1.2 mmol), **3a** (1.2 mmol), solvent (2 ml), reaction was monitored by TLC

<sup>a</sup>Determined by <sup>1</sup>H NMR analysis using CH<sub>2</sub>Br<sub>2</sub> as the internal standard

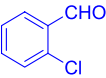
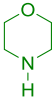
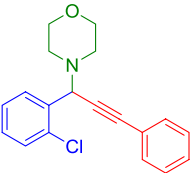
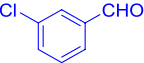
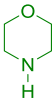
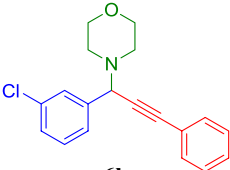
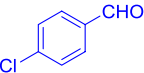
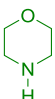
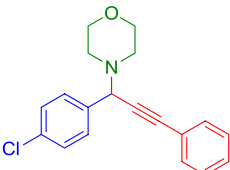
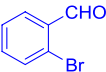
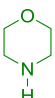
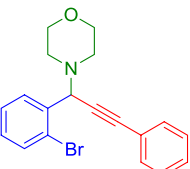
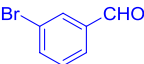
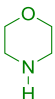
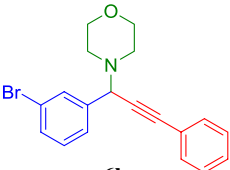
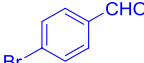
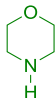
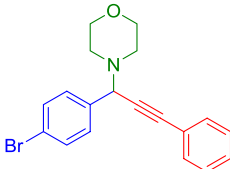
<sup>b</sup>The molar number of **1a**, **2a**, and **3a** is 1 mmol, 1.5 mmol, and 1.5 mmol

explored the effect of the molar ratio of the substrates on the model reaction. To our delight, the product yield increased from 53 to 60% by changing the substrates molar ratio of **1a**, **2a**, and **3** from 1/1.2/1.2 to 1/1.5/1.5 (Table 1, entries 13 and 14). Next, the effect of reaction temperature and time were examined on the model reaction. As shown from Table 1, increasing the reaction temperature to 110 °C and 120 °C, the product yields increased from 63 to 77%, respectively (Table 1, entries 15 and 16). At the same temperature, the best suitable time was found to be 12 h. Finally, the effect of amount of catalyst ranging from 5 to 10 mol% of Cu on the

**Table 2** Cu<sup>0</sup>NPs@CMC-catalyzed decarboxylative A3 coupling of phenylpropionic acid, aldehydes, and amines

1	2	3	6	
Entry	R <sub>1</sub> CHO	R <sub>2</sub> R <sub>3</sub> NH	Product	Yield <sup>a</sup> (%)
	1	2	6	
1				85
2				81
3				82
4				86
8				80
9				75

**Table 2** (continued)

Entry	R <sub>1</sub> CHO <b>1</b>	R <sub>2</sub> R <sub>3</sub> NH <b>2</b>	Product <b>6</b>	Yield <sup>a</sup> (%)
9			 <b>6g</b>	84
10			 <b>6h</b>	80
11			 <b>6i</b>	81
12			 <b>6j</b>	83
13			 <b>6k</b>	84
12			 <b>6l</b>	81

**Table 2** (continued)

Entry	R <sub>1</sub> CHO <b>1</b>	R <sub>2</sub> R <sub>3</sub> NH <b>2</b>	Product <b>6</b>	Yield <sup>a</sup> (%)
13				75
14				72
15				80
16				90
17				85
18				trace
19				trace

**Table 2** (continued)

Reaction conditions: **1** (1 mmol), **2** (1.5 mmol), **3** (1.5 mmol), 7.5 mol% Cu<sup>0</sup>NPs@CMC, 120 °C, 12 h under neat conditions

<sup>a</sup>Isolated yield

model was tested. Lowering the amount of the Cu to 5 mol% still allowed the reaction to proceed smoothly, decreasing the desired product **6a** in 53% yield respectively (Table 1, entry 17). However, a further increase of the catalyst to 10 mol% resulted in no improvement in yield at all (Table 1, entry 18).

With the optimized reaction conditions in hand, the scope of this decarboxylative coupling reaction of various aryl aldehydes **1**, amine **2**, and phenylpropionic acid **3** was explored, and the results are summarized in Table 2. In most cases, a range of aromatic aldehydes bearing electron-withdrawing group or electron-donating substituent afforded the corresponding products in moderate to excellent yields. These substituents have not apparent impact on the product yields. We next looked to expand the scope of aldehydes, and were delighted to find that aliphatic aldehydes could perform well. It is notable that the primary amines give no desired products.

Encouraged by these results of this decarboxylative coupling of aryl aldehyde, secondary amine, and phenylpropionic acid, we envisaged this catalyst is also practical in traditional A3 couplings under the similar optimal condition. Therefore, we further deployed the Cu<sup>0</sup>NPs@CMC catalyst in A3 coupling of aryl aldehyde **1**, secondary amines **2**, and phenylacetylene **4a**. The results listed in Table 3. As expected, all substrates afford the desired product in 77–92%. Generally, the traditional A3 reaction is commonly catalyzed by CuI catalysts, the results demonstrated that Cu<sup>0</sup>NPs@CMC nanocatalyst is also an efficient catalyst for this transformation.

The decarboxylative coupling of glyoxylic acid has been widely used as a valuable synthetic strategy for the synthesis of various molecules with a high density of functional groups. To achieve a more universal approach for the synthesis of propargylamines, we further expanded our method to a variety of decarboxylative A3 coupling reactions of glyoxylic acid **5**, phenylacetylenes **4**, and secondary amines **2** using Cu<sup>0</sup>NPs@CMC catalyst under similar conditions. The results listed in Table 4. Surprisingly, the Cu<sup>0</sup>NPs@CMC catalyst was also effective as using glyoxylic acid as an aldehyde source, which represents an elegant alternative for A3 coupling.

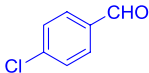
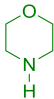
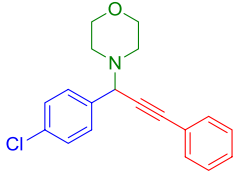
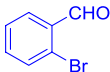
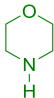
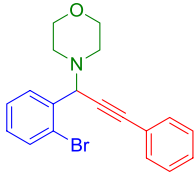
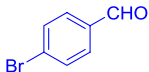
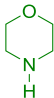
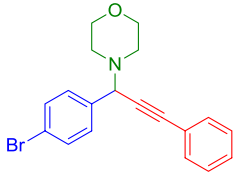
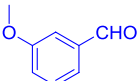
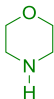
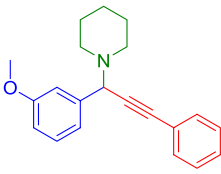
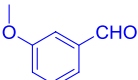
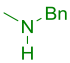
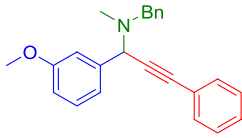
## Reusability of the catalyst

Recyclability of heterogeneous catalysts is important factor from the economical and sustainable chemistry stand points. Along this line we have studied recyclability of the catalyst for the model reaction of 4-methylbenzaldehyde **1a**, morpholine **2a**, and phenylpropionic acid **3** under optimized reaction conditions. After completion of the reaction, the Cu<sup>0</sup>NPs@CMC catalyst was recovered by simple filtration and reused in subsequent run. The results shown in Fig. 5 indicate that the Cu<sup>0</sup>NPs@CMC catalyst can be used for four consecutive cycles successfully with small drops in catalytic activity. The drop of catalytic activity seemed to be the loss of catalyst during the filtration process.

**Table 3** The traditional A3 couplings catalyzed by Cu<sup>0</sup>NPs@CMC nanocatalyst

Entry	R <sub>1</sub> CHO <b>1</b>	R <sub>2</sub> R <sub>3</sub> NH <b>2</b>	Product <b>6</b>	Yield <sup>a</sup> (%)
1				88
2				80
3				86
4				78
5				77
6				89

**Table 3** (continued)

Entry	R <sub>1</sub> CHO <b>1</b>	R <sub>2</sub> R <sub>3</sub> NH <b>2</b>	Product <b>6</b>	Yield <sup>a</sup> (%)
7			 <b>6i</b>	84
8			 <b>6j</b>	92
9			 <b>6l</b>	90
10			 <b>6d</b>	trace
11			 <b>6p</b>	85

Reaction conditions: **1** (1 mmol), **2** (1.2 mmol), **4a** (1.5 mmol), 7.5 mol% Cu<sup>0</sup>NPs@CMC, 100 °C, 5 h under neat conditions

<sup>a</sup>Isolated yield

A comparison of the efficiency and catalytic activity of the Cu<sup>0</sup>NPs@CMC catalyst with several previous documented methods is presented in Table 5. It turned



**Table 4** Cu<sup>0</sup>NPs@CMC-catalyzed decarboxylative A3 coupling of glyoxylic acid, phenylacetylenes and amines

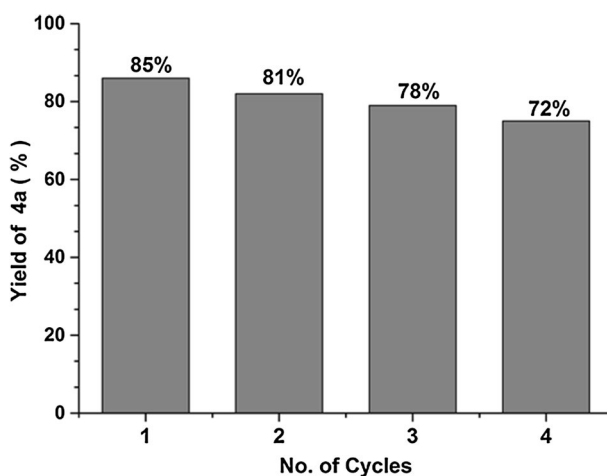
Entry	R <sub>2</sub> R <sub>3</sub> NH 2	phenylacetylene 4	Product 6	Yield <sup>a</sup> (%)
1				53
2				60
3				55
4				61
5				trace
6				70

**Table 4** (continued)

Entry	R <sub>2</sub> R <sub>3</sub> NH <b>2</b>	phenylacetylene <b>4</b>	Product <b>6</b>	Yield <sup>a</sup> (%)
7				72
8				65

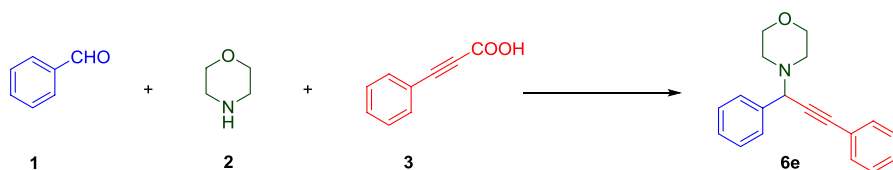
Reaction conditions: Reaction conditions: **5** (1 mmol), **2** (1.2 mmol), **4** (1.5 mmol), 7.5 mol% Cu<sup>0</sup>NPs@CMC, 110 °C, 15 h under neat conditions

<sup>a</sup>Isolated yield



**Fig. 5** Recyclability of Cu<sup>0</sup>NPs@CMC catalyst for the synthesis of **6a**

out that Cu<sup>0</sup>NPs@CMC catalyst gave comparable results than the other catalysts in terms of yield. In addition to this, stability, non-toxicity, and ease of separation and recycling are some obvious benefits with respect to the other methods.

**Table 5** A comparison on the efficiency of Cu<sup>0</sup>NPs@CMC with other reported methods in the synthesis of propargylamine via decarboxylative A3 coupling

Entry	Catalyst (mol%)	Solvent	Temp (°C)	Yield <sup>a</sup> (%)	Ref
1	Cu <sup>0</sup> NPs@CMC (7.5)	Neat	100	80	This work
2	CuI (10)	CH <sub>3</sub> CN	70	92	[47]
3	CuO/Fe <sub>2</sub> O <sub>3</sub> (5)	Neat	110	92	[52]
4	Chit@CuI(0.04)	Neat	140	83	[39]

## Conclusion

In conclusion, we have successfully developed a novel Cu<sup>0</sup>NPs@CMC nanocatalyst for the decarboxylative three-component coupling of an aryl aldehyde, a secondary amine, and a phenylpropionic acid, providing an efficient approach for the synthesis of polysubstituted propargylamines. Interestingly, the catalyst was also applicable to traditional A3 couplings as well as the decarboxylative three-component coupling of a glyoxylic acid, an amine, and an alkyne. Our method employs commercially available reagents and has significant advantages over the most reported copper decarboxylative A3 couplings and A3 couplings which usually require the use of nitrogen or phosphorus ligands, strong bases, and toxic solvents, in that it proceeds in neat under mild reaction conditions and displays a broad substrate scope and high yields. Therefore, this novel and efficient nanocatalyst can be regarded as a welcomed additional method for the existing catalysts generally applied to decarboxylative A3 and traditional A3 coupling reactions.

**Acknowledgements** We are grateful to the National Science Foundation of China (No. 21372099) and the Key Laboratory of Functional Molecular Engineering of Guangdong Province (2016kf06) for financial support.

## References

1. V.A. Peshkov, O.P. Pereshivko, A.A. Nechaev, A.A. Peshkov, E.V. Van der Eycken, *Chem. Soc. Rev.* **47**, 3861 (2018)
2. K. Lauder, A. Toscani, N. Scalacci, D. Castagnolo, *Chem. Rev.* **117**, 14091 (2017)
3. E. Vessally, L. Edjlali, A. Hosseini, A. Bekhradnia, M.D. Esrafil, *RSC Adv.* **6**, 49730 (2016)
4. C.E. Meyet, C.H. Larsen, *J. Org. Chem.* **79**, 9835 (2014)
5. S. Arshadi, E. Vessally, L. Edjlali, R. Hosseinzadeh-Khanmiri, E. Ghorbani-Kalhor, *Beilstein J. Org. Chem.* **13**, 625 (2017)
6. B.A. Orit, T. Amit, M.B. Youdim, O. Weinreb, *J. Neural Transm.* **123**, 125 (2016)
7. F.T. Zindo, J. Joubert, S.F. Malan, *Future Med. Chem.* **7**, 609 (2015)

8. K.B. Aubrecht, M.D. Winemiller, D.B. Collum, *J. Am. Chem. Soc.* **122**, 11084 (2000)
9. T. Murai, Y. Mutoh, Y. Ohta, M. Murakami, *J. Am. Chem. Soc.* **126**, 5968 (2004)
10. L. Zani, C. Bolm, *Chem. Commun.* **41**, 4263 (2006)
11. V.A. Peshkov, O.P. Pereshivko, E.V. Van der Eycken, *Chem. Soc. Rev.* **41**, 3790 (2012)
12. W.J. Yoo, L. Zhao, C.J. Li, *Aldrich. Acta* **44**, 43 (2011)
13. T.K. Saha, R. Das, *ChemistrySelect* **3**, 12206 (2018)
14. A. Beillard, T.X. Metro, X. Bantreil, J. Martinez, F. Lamaty, *Eur. J. Org. Chem.* **31**, 4642 (2017)
15. O. Prakash, H. Joshi, U. Kumar, A.K. Sharma, A.K. Singh, *Dalton Trans.* **44**, 1962 (2015)
16. M.T. Chen, B. Landers, O. Navarro, *Org. Biomol. Chem.* **10**, 2206 (2012)
17. C. Wei, C.J. Li, *J. Am. Chem. Soc.* **125**, 9584 (2003)
18. G.A. Price, A.K. Brisdon, K.R. Flower, R.G. Pritchard, P. Quayle, *Tetrahedron Lett.* **55**, 151 (2014)
19. V.K. Lo, Y. Liu, M.K. Wong, C.M. Che, *Org. Lett.* **8**, 1529 (2006)
20. P. Li, Y. Zhang, L. Wang, *Chem. Eur. J.* **15**, 2045 (2009)
21. W.W. Chen, R.V. Nguyen, C.J. Li, *Tetrahedron Lett.* **50**, 2895 (2009)
22. S. Layek, B. Agrahari, S. Kumari, Anuradha, D.D. Pathak, *Catal. Lett.* **148**, 2675 (2018)
23. M. Periasamy, P.O. Reddy, A. Edukondalu, M. Dalai, L.M. Alakonda, B. Udaykumar, *Eur. J. Org. Chem.* **27**, 6067 (2014)
24. E. Ramu, R. Varala, N. Sreelatha, S.R. Adapa, *Tetrahedron Lett.* **48**, 7184 (2007)
25. E.R. Bonfield, C.J. Li, *Org. Biomol. Chem.* **5**, 435 (2007)
26. A. Maleki, *Helv. Chim. Acta* **97**, 587 (2014)
27. M. Jeganathan, A. Dhakshinamoorthy, K. Pitchumani, *ACS Sustain. Chem. Eng.* **2**, 781 (2014)
28. N. Hussain, M.R. Das, *New J. Chem.* **41**, 12756 (2017)
29. L. He, Y. Liu, J. Liu, Y. Xiong, J. Zheng, Y. Liu, Z. Tang, *Angew. Chem. Int. Ed.* **52**, 3741 (2013)
30. K.S. Sindhu, G. Anilkumar, *RSC Adv.* **4**, 27867 (2014)
31. A. Grirrane, E. Alvarez, H. Garcia, A. Corma, *Angew. Chem. Int. Ed.* **53**, 7253 (2014)
32. V.S. Kashid, M.S. Balakrishna, *Catal. Commun.* **103**, 78 (2018)
33. Q. Zhang, J.X. Chen, W.X. Gao, J.C. Ding, H.Y. Wu, *Appl. Organomet. Chem.* **24**, 809 (2010)
34. J.R. Cammarata, R. Rivera, F. Fuentes, Y. Otero, E. Ocando-Mavárez, A. Arce, J.M. Garcia, *Tetrahedron Lett.* **58**, 4078 (2017)
35. Y. Ju, C.J. Li, R.S. Varma, *QSAR Comb. Sci.* **23**, 891 (2004)
36. N. Bahri-Laleh, S. Sadjadi, *Res. Chem. Intermed.* **44**, 6351 (2018)
37. J. Safaei-Ghomi, S.H. Nazemzadeh, H. Shahbazi-Alavi, *Res. Chem. Intermed.* **43**, 7375 (2017)
38. X. Liu, B. Lin, Z. Zhang, H. Lei, Y. Li, *RSC Adv.* **6**, 94399 (2016)
39. P. Kaur, B. Kumar, V. Kumar, R. Kumar, *Tetrahedron Lett.* **59**, 1986 (2018)
40. M.J. Albaladejo, F. Alonso, Y. Moglie, M. Yus, *Eur. J. Org. Chem.* **16**, 3093 (2012)
41. S. Frindy, A. El Kadib, M. Lahcini, A. Primo, H. García, *Catal. Sci. Technol.* **6**, 4306 (2016)
42. M. Gholinejad, F. Saadati, S. Shaybanizadeh, B. Pullithadathil, *RSC Adv.* **6**, 4983 (2016)
43. V.G. Ramu, A. Bordoloi, T.C. Nagaiah, W. Schuhmann, M. Muhler, C. Cabrele, *Appl. Catal. A* **431–432**, 88 (2012)
44. M. Kidwai, V. Bansal, N.K. Mishra, A. Kumar, S. Mozumdar, *Synlett* **2007**, 1581 (2007)
45. D.S. Ermolat'ev, H. Feng, G. Song, E.V. Van der Eycken, *Eur. J. Org. Chem.* **24**, 5346 (2014)
46. J. Choi, J. Lim, F.M. Irudayanathan, H. Kim, J. Park, S.B. Yu, Y. Jang, G.C.E. Raja, K.C. Nam, J. Kim, S. Lee, *Asian J. Org. Chem.* **5**, 770 (2016)
47. J. Lim, K. Park, A. Byeun, S. Lee, *Tetrahedron Lett.* **55**, 4875 (2014)
48. H. Feng, D.S. Ermolat'ev, G. Song, E.V. Van der Eycken, *Org. Lett.* **14**, 1942 (2012)
49. H. Feng, D.S. Ermolat'ev, G. Song, E.V. Van der Eycken, *J. Org. Chem.* **76**, 7608 (2011)
50. P. Zhao, H. Feng, H. Pan, Z. Sun, M. Tong, *Org. Chem. Front.* **4**, 37 (2017)
51. T. Palani, K. Park, M.R. Kumar, H.M. Jung, S. Lee, *Eur. J. Org. Chem.* **26**, 5038 (2012)
52. U. Gulati, U.C. Rajesh, D.S. Rawat, *Tetrahedron Lett.* **57**, 4468 (2016)
53. U.C. Rajesh, U. Gulati, D.S. Rawat, *ACS Sustain. Chem. Eng.* **4**, 3409 (2016)
54. U. Gulati, U.C. Rajesh, N. Bunekar, D.S. Rawat, *ACS Sustain. Chem. Eng.* **5**, 4672 (2017)
55. M.N. Nadagouda, R.S. Varma, *Biomacromol* **8**, 2762 (2007)
56. J. Xiao, Z. Lu, Y. Li, *Ind. Eng. Chem. Res.* **54**, 790 (2015)
57. Z. Zhang, P. Song, J. Zhou, Y. Chen, B. Lin, Y. Li, *Ind. Eng. Chem. Res.* **55**, 12301 (2016)
58. B. Lin, X. Liu, Z. Zhang, Y. Chen, X. Liao, Y. Li, *J. Colloid Interf. Sci.* **497**, 134 (2017)
59. Z. Zhang, Y. Zhang, X. Liu, B. Shen, T. Zhang, Y. Li, *Appl. Organomet. Chem.* **31**, e3912 (2017)
60. Y. Chen, T. Zhang, D. Wang, J. Zhou, Y. Zhang, Y. Li, *J. Chem. Sci.* **129**, 421 (2017)

61. F. He, D. Zhao, J. Liu, C.B. Roberts, *Ind. Eng. Chem. Res.* **46**, 29 (2007)
62. J. Liu, F. He, E. Durham, D. Zhao, C.B. Roberts, *Langmuir* **24**, 328 (2008)
63. K. Wang, L. Yang, W. Zhao, L. Cao, Z. Sun, F. Zhang, *Green Chem.* **19**, 1949 (2017)
64. K.R. Reddy, N.S. Kumar, B. Sreedhar, M.L. Kantam, *J. Mol. Catal. A Chem.* **252**, 136 (2006)

**Publisher's Note** Springer Nature remains neutral with regard to jurisdictional claims in published maps and institutional affiliations.

## Affiliations

Xiaoping Liu<sup>1</sup> · Xiaobin Tan<sup>1</sup> · Yuemin Zhou<sup>1</sup> · Yiqun Li<sup>1,2</sup> · Zhubao Zhang<sup>1</sup>

<sup>1</sup> Department of Chemistry, Jinan University, Guangzhou 510632, People's Republic of China

<sup>2</sup> Key Lab of Functional Molecular Engineering of Guangdong Province, South China University of Technology, Guangzhou 510640, People's Republic of China